

ORB-SLAM: a Versatile and Accurate Monocular SLAM System

Raúl Mur-Artal*, J. M. M. Montiel, and Juan D. Tardós

Abstract—The gold standard method for tridimensional reconstruction and camera localization from a set of images is well known to be Bundle Adjustment (BA). Although BA was regarded for years as a costly method restricted to the offline domain, several real time algorithms based on BA flourished in the last decade. However those algorithms were limited to perform SLAM in small scenes or only Visual Odometry. In this work we built on excellent algorithms of the last years to design from scratch a Monocular SLAM system that operates in real time, in small and large, indoor and outdoor environments, with the capability of wide baseline loop closing and relocalization, and including full automatic initialization. Our *survival of the fittest* approach to select the points and keyframes of the reconstruction generates a compact and trackable map that only grows if the scene content changes, enhancing lifelong operation. We present an exhaustive evaluation in 27 sequences from the most popular datasets achieving unprecedented performance with a typical localization accuracy from 0.2% to 1% of the trajectory dimension in scenes from a desk to several city blocks. We make public a ROS implementation.

Index Terms—Lifelong Mapping, Localization, Monocular Vision, Recognition, SLAM

I. INTRODUCTION

BUNDLE ADJUSTMENT (BA) is known to be the optimal method to estimate camera localization and a sparse geometrical reconstruction of a scene from a set of images [1], [2]. For long time this approach was considered not affordable for a robot to reconstruct in real time its environment and localise itself in it (SLAM). To achieve accurate results at non-prohibitive computational cost, a real time SLAM algorithm has to provide BA with:

- Corresponding observations of scene features (map points) among a subset of selected frames (keyframes).
- As complexity is cubic in the number of keyframes, their selection should avoid unnecessary redundancy.
- A strong network configuration of keyframes and points to produce accurate results, that is, a well spread set of keyframes observing points with significant parallax and with plenty of loop closure matches.
- An initial estimation of the keyframe poses and point locations for the non-linear optimization.

The first real time SLAM algorithm based on BA was the ground breaking work of Klein and Murray [3], known as Parallel Tracking and Mapping (PTAM). This algorithm

provided simple but effective methods for keyframe selection, feature matching, point triangulation, camera localization for every frame and relocalization after tracking failure. Nevertheless PTAM had several limitations as the lack of a loop closing mechanism, the low invariance to viewpoint of its relocalization method, the need of human intervention for map initialization, and its restriction to small scenes.

In this work we build on the main ideas of PTAM, the loop detection work of Gálvez-López and Tardós [4], the scale-aware loop closing method of Strasdat et. al [5] and their idea of a local covisible map for large scale operation [6], to design a new Monocular SLAM system from scratch that overcomes the limitations of PTAM. Our system has the following properties:

- Use of the same ORB [7] features for tracking, mapping and place recognition based on bags of words. ORB are extremely fast to compute and match without the need of GPU or multi-threading, being invariant to rotation and scale (in a certain range).
- Real time operation in large environments, thanks to the use of a covisibility graph to focus tracking and mapping operations in a local covisible area, independent of global map size.
- Real time loop closing based on the optimization of a pose graph that we call the *Essential Graph*, which is built from a spanning tree that is maintained by the system, the loop closure links and some strong edges from the covisibility graph.
- Real time camera relocalization with high invariance to viewpoint.
- A new automatic and robust initialization procedure based on model selection that permits to create an initial map from planar and non-planar scenes.
- A *survival of the fittest* approach to map point and keyframe selection that is little conservative in the spawning but very restrictive in the culling. This improves tracking robustness as many keyframes are created under hard conditions in exploration (i.e. strong rotations), while the culling allows to maintain a compact reconstruction of the scene as redundant keyframes are not retained, which enhances lifelong operation.

We perform an extensive evaluation in popular public datasets from indoor and outdoor environments, including hand-held, car and robot sequences. Surprisingly we achieve better camera localization accuracy than the state of the art in direct methods [8], which optimize directly over pixel intensities instead of feature reprojection errors. We perform a discussion in Section IX-B of the possible causes that can

This work was supported by the Dirección General de Investigación of Spain under Project DPI2012-32168, the Ministerio de Educación Scholarship FPU13/04175 and Gobierno de Aragón Scholarship B121/13.

The authors are with the Instituto de Investigación en Ingeniería de Aragón (I3A), Universidad de Zaragoza, María de Luna 1, 50018 Zaragoza, Spain (e-mail: raulmur@unizar.es; josemari@unizar.es; tardos@unizar.es).

*Corresponding author.

make feature-based more accurate than direct methods. To the best of our knowledge this is the most complete and reliable solution to Monocular SLAM, and to the benefit of the community we release a ROS implementation. The code and demonstrating videos can be found in our project webpage.¹ The loop closing and relocalization methods here presented are based on our previous work [9]. A rough preliminary version of the system was presented in [10]. In the current paper we include the initialization method, the *Essential Graph*, and perfect all methods involved. We also describe in detail all building blocks and perform an exhaustive experimental validation.

II. RELATED WORK

We start reviewing the evolution of Place Recognition, which is essential for loop detection and relocalization. We then discuss map initialization approaches for Monocular SLAM and end with a review of Monocular SLAM systems.

A. Place Recognition

The survey by Williams et al. [11] compared several approaches for place recognition and concluded that techniques based on appearance, that is image to image matching, scale better in large environments than map to map or image to map methods. Within appearance based methods, bags of words techniques [12], such as the probabilistic approach FAB-MAP [13], are to the fore because of their high efficiency. DBoW2 [4] used for the first time bags of binary words obtained from BRIEF descriptors [14] along with the very efficient FAST feature detector [15], reducing in more than one order of magnitude the time needed for feature extraction, compared to SURF [16] and SIFT [17] features that were used in bags of words approaches so far. Although the system demonstrated to be very efficient and robust, the use of BRIEF, neither rotation nor scale invariant, limited the system to in-plane trajectories and loop detection from similar viewpoints. In our previous work [9], we proposed a bag of words place recognizer built on DBoW2 with ORB [7], which are binary features invariant to rotation and scale (in a limited range), resulting in a very fast recognizer with high invariance to viewpoint. We demonstrated the high recall and robustness of the recognizer in four different datasets, requiring less than 39 ms (including feature extraction) to retrieve a loop candidate from a 10K image database. In this work we use an improved version of that place recognizer, using covisibility information and returning several hypotheses when querying the database instead of just the best match.

B. Map Initialization

Monocular SLAM requires a procedure to create an initial map because depth cannot be recovered from a single image. One way to solve the problem is to initially track a known structure [18]. In the context of filtering approaches, points can be initialized with high uncertainty in depth using an inverse depth parametrization [19], which hopefully will later

converge to their real positions. The recent semi-dense work of Engels et. al [8], follows a similar approach initializing the depth of the pixels to a random value with high variance.

Initialization methods from two views either assumes locally scene planarity [3], [20] and recover the relative camera pose from a homography using the method of Faugeras et. al [21], or compute an essential matrix [22], [23] that models planar and general scenes, using the five-point algorithm of Nister [24], which requires to deal with multiple solutions. Both reconstruction methods are not well constrained under low parallax and suffer from a twofold ambiguity solution if all points of a planar scene are closer to one of the camera centers [25]. On the other hand if a non-planar scene is seen with parallax a unique fundamental matrix can be computed and the relative camera pose can be recovered without ambiguity.

We present in Section IV a new automatic approach based on model selection between a homography for planar scenes and a fundamental matrix for non-planar scenes. A statistical approach to model selection was proposed by Torr et al. [26]. Under a similar rationale we have developed a heuristic initialization algorithm that takes into account the risk of selecting a fundamental matrix in close to degenerate cases (i.e. planar, nearly planar, and low parallax), favoring the selection of the homography. In the planar case, for the sake of safe operation, we refrain from initializing if the solution has a twofold ambiguity, as a corrupted solution could be selected. We delay the initialization until the method produces a unique solution with significant parallax.

C. Monocular SLAM

Monocular SLAM was initially solved by filtering [18], [19], [27]. In that approach every frame is processed by the filter to jointly estimate the map feature locations and the camera pose. It has the drawbacks of wasting computation in processing consecutive frames with little new information and the accumulation of linearization errors. On the other hand keyframe-based approaches [3] estimate the map using only selected frames, called keyframes, allowing to perform more costly but accurate bundle adjustment optimizations, as mapping is not tied to frame-rate. Strasdat et. al [28] demonstrated that keyframe-based techniques are more accurate than filtering for the same computational cost.

The most representative keyframe-based SLAM system is probably PTAM by Klein and Murray [3]. It was the first work to introduce the idea of splitting camera tracking and mapping in parallel threads, and demonstrated to be successful for real time augmented reality applications in small environments. The original version was later improved with edge features, a rotation estimation step during tracking and a better relocalization method [29]. PTAM has become a standard in monocular vision, and it has been recently adapted for MAVs navigation [30], [31]. The map points of PTAM correspond to FAST corners matched by patch correlation. This makes the points only useful for tracking but not for place recognition. In fact PTAM does not detect large loops, and the relocalization is based on the correlation of low resolution thumbnails of the keyframes, yielding a low invariance to viewpoint.

¹<http://webdiis.unizar.es/~raulmur/orbslam>

Strasdat et. al [6] used the front-end of PTAM in their double window optimization approach. They built a covisibility graph of keyframes that allows to retrieve a local map that will be used for tracking instead of projecting the whole map as original PTAM does. They also included a loop detection mechanism based on bags of words with SURF features, but as they use different features for tracking and loop detection, they need to estimate the depth of the SURF features using interpolation. Scale drift was considered including similarity constraints [5] in the pose-pose constraints of the outer window in the optimization. However loop closing is only effective if the size of the outer window is large enough to include the whole loop. We take advantage in our system of the excellent ideas of the local map based on covisibility and the loop closing with scale-drift correction.

Pirker et. al [32] proposed CD-SLAM, with completely different mapping and tracking methods from PTAM, designed to work in dynamic environments. Instead of using FAST points and patch search like PTAM tracking, CD-SLAM uses SIFT features and GPU acceleration for real-time matching. This system uses also covisibility information between keyframes but also on the map points to select which points to search during tracking, enabling large scale operation. Loop detection and relocalization use FAB-MAP [13]. The loop closing is based on pose graph optimization [5] followed by structure-only bundle adjustment. This system was very complete including loop closing, relocalization, large scale operation and efforts to work on dynamic environments. However map initialization is not mentioned. The lack of a public implementation does not allow us to perform a comparison of accuracy, robustness or large-scale capabilities.

The recent work of Lim et. al [23] was published after we submitted our preliminary version of this work [10], and as in our work, they use the same features for tracking, mapping and loop detection. However the choice of BRIEF features limits the system to in-plane trajectories. Their system only tracks points from the last keyframe so the map is not reused if revisited (similar to visual odometry) and has the problem of growing unbounded. In contrast, our system tracks a local map of many keyframes, which includes the keyframes previously created in the place that is being revisited, effectively reusing the map. In addition our system maintains the map bounded thanks to our keyframe culling policy. We compare qualitatively our results with this approach in section VIII-E.

In the recent work of Engel et. al [8], known as LSD-SLAM, they are able to build large scale semi-dense maps, using direct methods (i.e. optimization directly over image pixel intensities) instead of bundle adjustment over features. Their results are very impressive as they are able to operate in real time, without GPU acceleration, building a semi dense map, which is more useful for robotics than the sparse output generated by feature-based SLAM approaches as ours. Nevertheless they still need features for loop detection and their camera localization accuracy is significantly lower than in our system and PTAM, as we show experimentally in Section VIII-B. This surprising result is discussed in Section IX-B.

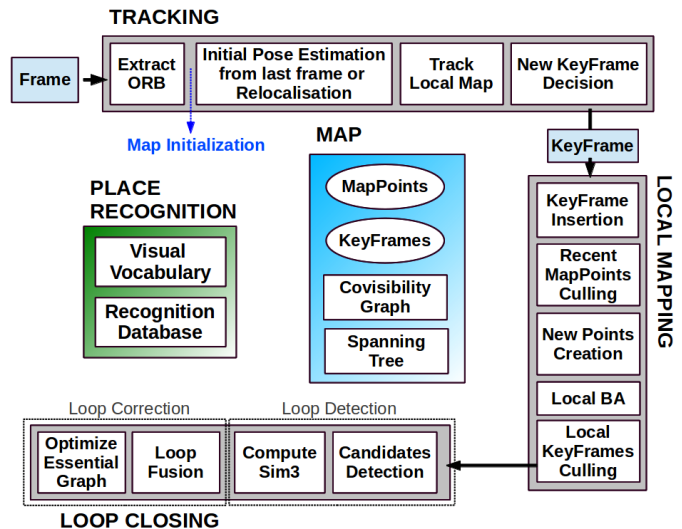


Fig. 1. ORB-SLAM system overview, showing all the steps performed by the tracking, local mapping and loop closing threads. The main components of the place recognition module and the map are also shown.

III. SYSTEM OVERVIEW

Our SLAM system incorporates three threads that run in parallel: the tracking, the local mapping and the loop closing. Fig. 1 shows an overview of the system. One of the main properties of the system is that the same ORB features [7] that are triangulated by the mapping and tracked by the tracking are used for place recognition to perform loop detection and relocalization. ORB features are oriented multi-scale FAST corners with a 256 bits descriptor associated. As binary features, they are extremely fast to compute and match, while they are highly invariant to viewpoint. This allows to match them from wide baselines, boosting the accuracy of BA.

The tracking thread is in charge of localising the camera with every frame and deciding when to insert a new keyframe. We use a constant velocity motion model to roughly predict the new camera pose and then perform an initial matching with the previous frame. If the tracking is lost (e.g. due to occlusions, abrupt movement), the place recognition module is used to perform a global relocalization. Once there is an initial estimation of the camera pose and feature matching, a local visible map is retrieved using the covisibility graph of keyframes that is maintained by the system. Then matches with the local map points are searched by reprojection, and camera pose is optimized using motion-only BA (i.e. points are fixed). Finally the tracking thread decides if a new keyframe is inserted. The main novelties of our approach are that the relocalization is fully embedded in the tracking procedure, and that the keyframe insertion policy is generous as the keyframe culling procedure in the local mapping thread will later discard redundant keyframes. This boost the tracking robustness under hard exploring conditions (i.e. rotations, fast movements) as keyframes are inserted every few frames. All the tracking steps are explained in detail in Section V. The novel procedure to create an initial map is presented in Section IV.

The local mapping thread processes new keyframes and performs local bundle adjustment to achieve an optimal re-

construction in the surroundings of the camera pose. New correspondences for unmatched ORB in the new keyframe are searched in connected keyframes in the covisibility graph to triangulate new points. Some time after creation, based on the information gathered during the tracking, an exigent point culling policy is applied in order to retain only high quality points. The local mapping is also in charge of culling redundant keyframes, which in conjunction with the generous spawning policy of the tracking completes our keyframe selection strategy. We explain in detail all local mapping steps in Section VI.

The loop closing thread searches for large loops with every new keyframe. If a loop is detected, a similarity transformation that informs about the drift accumulated in the loop is computed. Then both sides of the loop are aligned and duplicated points are fused. Finally a pose graph optimization over similarity constraints [5] is performed to achieve global consistency. The main novelty is that we perform the optimization over a sparser subgraph of the covisibility graph, but retaining a strong camera network, that we call the *Essential Graph*, which is explained in Section III-B. The loop detection and correction steps are explained in detail in Section VII.

All optimizations performed in the system are carried out by the optimization framework g2o [33]. It must be also said that in our C++ implementation, we took care to incorporate mutex at the level of objects to guarantee a safe multi-thread operation. Next we describe the main entities that compose our system: map points, keyframes, the covisibility graph, the essential graph, and the place recognition module.

A. Map Points, KeyFrames and their Management

Each map point p_i stores:

- Its 3D position $\mathbf{X}_{w,i}$ in the world coordinate system.
- The viewing direction \mathbf{n}_i , which is the mean unit vector of all its viewing directions (the rays that join the point with the keyframe optical centers that observe it).
- A representative ORB descriptor \mathbf{D}_i , which is the associated ORB descriptor whose hamming distance is minimum with respect to all other associated descriptors in the keyframes in which the point is observed.
- The maximum d_{\max} and minimum d_{\min} distances at which the point can be observed, according to the scale invariance limits of the ORB features.

Each keyframe K_i stores:

- The camera pose \mathbf{T}_{iw} , which is a rigid body transformation that transforms points from the world to the camera coordinate system.
- The camera intrinsics, including focal length and principal point.
- All the ORB features extracted in the frame, associated or not to a map point, whose coordinates are undistorted if a distortion model is provided.

Map points and keyframes are created with a generous policy, while a later very exigent culling mechanism is in charge of detecting redundant keyframes and wrongly matched or not trackable map points. This permits a flexible map

expansion during exploration, while its size is bounded under continual revisits of the same environment, i.e. lifelong operation. Additionally our maps contain very few outliers compared with PTAM, at the expense of containing less points. Culling procedures of map points and keyframes are explained in Sections VI-B and VI-E respectively.

B. Covisibility Graph and Essential Graph

Covisibility information between keyframes is very useful in several tasks of our system, and is represented as an undirected weighted graph as in [6]. Each node is a keyframe and an edge between two keyframes exists if they share observations of the same map points, being the weight of the edge the number of common map points. Strasdat et. al [6] impose a minimum weight θ_{\min} between 15 and 30 to include an edge in the covisibility graph. We propose to build a base graph without weight restriction and then depending on the task, retrieve a subgraph imposing a θ_{\min} . Modifying θ_{\min} we can control how interconnected is the subgraph.

In order to correct a loop we perform a pose graph optimization that distributes the loop closing error along the graph. In order not to include all the edges provided by the covisibility graph, which can be very dense, we propose to build an *Essential Graph* that retains all the nodes (keyframes), but less edges, still preserving a strong network that yields accurate results. The system builds incrementally a spanning tree from the initial keyframe, which provides a connected subgraph of the covisibility graph with minimal number of edges. When a new keyframe is inserted, it is included in the tree linked to the keyframe which shares most point observations, and when a keyframe is erased by the culling policy, the system updates the links affected by that keyframe. The *Essential Graph* contains the spanning tree, the subset of edges from the covisibility graph with high covisibility ($\theta_{\min} = 100$), and the loop closure edges, resulting in a strong network of cameras. As shown in the experiments of Section VIII-E, when performing the pose graph optimization, the solution is so accurate that an additional full bundle adjustment optimization barely improves the solution.

C. Bags of Words Place Recognition

The system has embedded a bags of words place recognition module to perform loop detection and relocalization. Visual words are just a discretization of the descriptor space, which is known as the visual vocabulary. The vocabulary is created offline with the ORB descriptors extracted from a large set of images. If the images are general enough, the same vocabulary can be used for different environments getting a good performance, as demonstrated in our previous work [9]. The system builds incrementally a database that contains an invert index, which stores for each visual word in the vocabulary, in which keyframes it has been seen, so that querying the database can be done very efficiently. The database is also updated when a keyframe is deleted by the culling procedure.

Because there exists visual overlap between keyframes, when querying the database there will not exist a unique keyframe with a high score. DBoW2 [4] took this overlapping

into account, adding up the score of images that are close in time. This has the limitation of not including keyframes viewing the same place but inserted at a different time. Instead we group those keyframes that are connected in the covisibility graph. The database query returns all keyframe matches whose scores are higher than the 75% of the best score.

An additional benefit of the bags of words representation for feature matching was reported in [4]. When we want to compute the correspondences between two sets of ORB features, we can constraint the brute force matching only to those features that belong to the same node in the vocabulary tree at a certain level (we select the second out of six), speeding up the search. We use this *trick* when searching matches for triangulating new points, and at loop detection and relocalization. We also refine the correspondences with an orientation consistency test, see [9] for details, that discard outliers ensuring a coherent rotation for all correspondences.

IV. AUTOMATIC MAP INITIALIZATION

The goal of the map initialization is to compute the relative pose between two frames to triangulate an initial set of map points. This method should be independent of the scene (planar or general) and should not require human intervention to select a good two-view configuration, i.e. a configuration with significant parallax. We propose to compute in parallel two geometrical models, a homography assuming a planar scene and a fundamental matrix assuming a non-planar scene. We then use a heuristic to select a model and try to recover the relative pose with a specific method for the selected model. Our method only initializes when it is certain that the two-view configuration is safe, detecting low-parallax cases and the well-known twofold planar ambiguity [25], avoiding to initialize a corrupted map. The steps of our algorithm are:

- 1) Find initial correspondences:

Extract ORB features (only at the finest scale) in the current frame F_c and search for matches $\mathbf{x}_c \leftrightarrow \mathbf{x}_r$ in the reference frame F_r . If not enough matches are found, reset the reference frame.

- 2) Parallel computation of the two models:

Compute in parallel threads a homography \mathbf{H}_{cr} and a fundamental matrix \mathbf{F}_{cr} :

$$\mathbf{x}_c = \mathbf{H}_{cr} \mathbf{x}_r \quad \mathbf{x}_c^T \mathbf{F}_{cr} \mathbf{x}_r = 0 \quad (1)$$

with the normalized DLT and 8-point algorithms respectively as explained in [2] inside a RANSAC scheme. To make homogeneous the procedure for both models, the number of iterations is prefixed and the same for both models, along with the points to be used at each iteration, 8 for the fundamental matrix, and 4 of them for the homography. At each iteration we compute a score S_M for each model M (H for the homography, F for the fundamental matrix):

$$S_M = \sum_i (\rho_M(d_{cr,M}^2(\mathbf{x}_c^i, \mathbf{x}_r^i)) + \rho_M(d_{rc,M}^2(\mathbf{x}_c^i, \mathbf{x}_r^i)))$$

$$\rho_M(d^2) = \begin{cases} \Gamma - d^2 & \text{if } d^2 < T_M \\ 0 & \text{if } d^2 \geq T_M \end{cases} \quad (2)$$

where d_{cr}^2 and d_{rc}^2 are the symmetric transfer errors [2] from one frame to the other. T_M is the outlier rejection threshold based on the χ^2 test at 95% ($T_H = 5.99$, $T_F = 3.84$). Γ is defined equal to T_H so that both models score equally for the same d in their inlier region, again to make the process homogeneous.

We keep the homography and fundamental matrix with highest score. If no model could be found (not enough inliers), we restart the process again from step 1.

- 3) Model selection:

If the scene is planar, nearly planar or there is low parallax, it can be explained by a homography. However a fundamental matrix can also be found, but the problem is not well constrained [2] and any attempt to recover the motion from the fundamental matrix would yield wrong results. We should select the homography as the reconstruction method will correctly initialize from a plane or it will detect the low parallax case and refuse the initialization. On the other hand a non-planar scene with enough parallax can only be explained by the fundamental matrix, but a homography can also be found explaining a subset of the matches if they lie on a plane or they have low parallax (they are far away). In this case we should select the fundamental matrix. We have found that a robust heuristic is to compute:

$$R_H = \frac{S_H}{S_H + S_F} \quad (3)$$

and select the homography if $R_H > 0.45$, which adequately captures the planar and low parallax cases. Otherwise, we select the fundamental matrix.

- 4) Motion and Structure from Motion recovery:

Once a model is selected we retrieve the motion hypotheses associated. In the case of the homography we retrieve 8 motion hypotheses using the method of Faugeras et. al [21]. The method propose cheriality tests to select the valid solution. However these tests fail if there is low parallax as points easily go in front or back of the cameras, which could yield the selection of a wrong solution. We propose to directly triangulate the eight solutions, and check if there is one solution with most points seen with parallax, in front of both cameras and with low reprojection error. If there is not a clear winner solution, we do not initialize and continue from step 1. This technique to disambiguate the solutions makes our initialization robust under low parallax and the twofold ambiguity configuration, and could be considered the key of the robustness of our method.

In the case of the fundamental matrix, we convert it in an essential matrix using the calibration matrix \mathbf{K} :

$$\mathbf{E}_{rc} = \mathbf{K}^T \mathbf{F}_{rc} \mathbf{K} \quad (4)$$

and then retrieve 4 motion hypotheses with the singular value decomposition method of [2]. We must ensure the determinant of the rotations to be 1, as explained in [34]. We then triangulate the four solutions and select the reconstruction as done for the homography.

5) Bundle adjustment:

If we have found a reconstruction, we then perform bundle adjustment to refine the initial map.

An example of a challenging initialization in the outdoor NewCollege robot sequence [35] is shown in Fig. 2. It can be seen how PTAM and LSD-SLAM have initialized all points in a plane, while our method has waited until there is enough parallax, initializing correctly from the fundamental matrix.

V. TRACKING

In this section we describe the steps of the tracking thread that are performed with every frame from the camera. Camera pose optimizations consists in motion-only BA (i.e. points are fixed) using the Levenberg-Marquadt method implemented in g2o [33] and the Huber robust cost function.

A. ORB extraction

We extract FAST corners at 8 scale levels with a scale factor of 1.2. For image resolutions from 512×384 to 752×480 pixels we found suitable to extract 1000 corners, for higher resolutions, as the 1241×376 in the KITTI dataset [36] we extract 2000 corners. In order to ensure an homogeneous distribution we divide each scale level in a grid, trying to extract at least 5 corners per cell. Then we detect corners in each cell, adapting the detector threshold if not enough corners are found. The amount of corners retained per cell is also adapted if some cells contains no corners (textureless or low contrast). The orientation and ORB descriptor are then computed on the retained FAST corners.

B. Initial Pose Estimation from previous frame

If tracking was successful for last frame, we use a constant velocity motion model to predict the camera pose and perform a guided search of the map points observed in the last frame. If not enough matches were found (i.e. motion model is clearly violated), we use a wider search of the map points around their position in the last frame. The pose is then optimized with the found correspondences.

C. Initial Pose Estimation via Global Relocalization

If the tracking is lost, we convert the frame into bag of words and query the recognition database for keyframe candidates for global relocalization. We compute correspondences with ORB associated to map points in each keyframe, as explained in section III-C. We then perform alternatively RANSAC iterations for each keyframe and try to find a camera pose using the PnP algorithm [37]. If we find a camera pose with enough inliers, we optimize the pose and perform a guided search of more matches with the map points of the candidate keyframe. Finally the camera pose is again optimized, and if supported with enough inliers, tracking procedure continues.

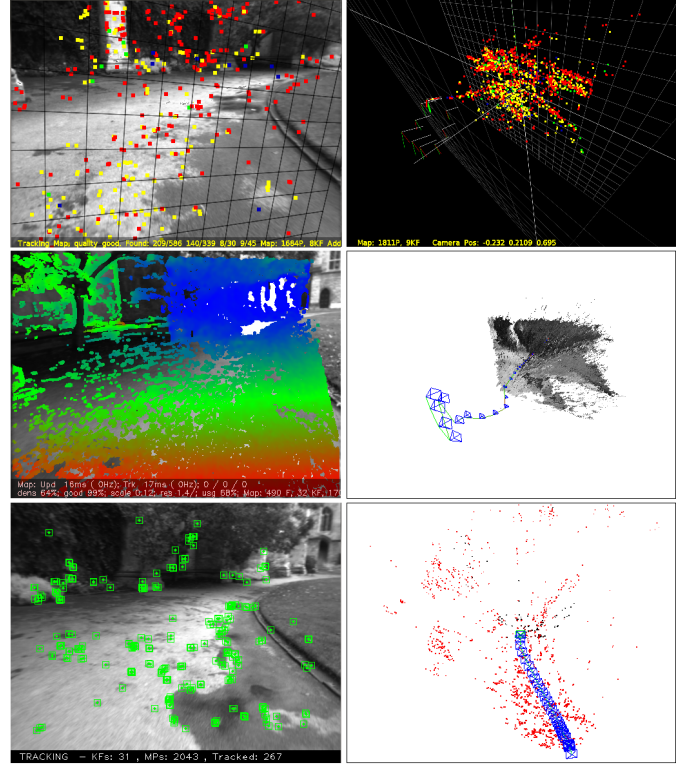


Fig. 2. Top: PTAM, middle LSD-SLAM, bottom: ORB-SLAM, some time after initialization in the NewCollege sequence [35]. PTAM and LSD-SLAM initialize a corrupted planar solution while our method has automatically initialized from the fundamental matrix when it has detected enough parallax. Depending on which keyframes are manually selected, PTAM is also able to initialize well.

D. Track Local Map

Once we have an estimation of the camera pose and an initial set of feature matches, we can project the map into the frame and search more map point correspondences. To bound the complexity in large maps, we only project a local map. This local map contains the set of keyframes \mathcal{K}_1 , that share map points with the current frame, and a set \mathcal{K}_2 with neighbors to the keyframes \mathcal{K}_1 in the covisibility graph. The local map also has a reference keyframe $K_{\text{ref}} \in \mathcal{K}_1$ which shares most map points with current frame. Now each map point seen in \mathcal{K}_1 and \mathcal{K}_2 is searched in the current frame as follows:

- 1) Compute the map point projection \mathbf{x} in the current frame. Discard if it lays out of the image bounds.
- 2) Compute the angle between the current viewing ray \mathbf{v} and the map point mean viewing direction \mathbf{n} . Discard if $\mathbf{v} \cdot \mathbf{n} < \cos(60^\circ)$.
- 3) Compute the distance d from map point to camera center. Discard if it is out of the scale invariance region of the map point $d \notin [d_{\min}, d_{\max}]$.
- 4) Compute the scale in the frame by the ratio d/d_{\min} .
- 5) Compare the representative descriptor \mathbf{D} of the map point with the still unmatched ORB features in the frame, at the predicted scale, and near \mathbf{x} , and associate the map point with the best match.

The camera pose is finally optimized with all the map points found in the frame.

E. New Keyframe Decision

The last step is to decide if the current frame is spawned as a new keyframe. As there is a mechanism in the local mapping to cull redundant keyframes, we will try to insert keyframes as fast as possible, because that makes the tracking more robust to challenging camera movements, typically rotations. To insert a new keyframe all the following conditions must be met:

- 1) More than 20 frames must have passed from the last global relocalization.
- 2) Local mapping is idle, or more than 20 frames have passed from last keyframe insertion.
- 3) Current frame tracks at least 50 points.
- 4) Current frame tracks less than 90% points than K_{ref} .

Instead of using a distance criterium to other keyframes as PTAM, we impose a minimum visual change (condition 4). Condition 1 ensures a good relocalization and condition 3 a good tracking. If a keyframe is inserted when the local mapping is busy (second part of condition 2), a signal is sent to stop local bundle adjustment, so that it can process as soon as possible the new keyframe.

VI. LOCAL MAPPING

In this section we describe the steps performed by the local mapping with every new keyframe K_i .

A. KeyFrame Insertion

At first we update the covisibility graph, adding a new node for K_i and updating the edges resulting from the shared map points with other keyframes. We then update the spanning tree linking K_i with the keyframe with most points in common. We then compute the bags of words representation of the keyframe, that will help in the data association for triangulating new points.

B. Recent Map Points Culling

Map points, in order to be retained in the map, must pass a restrictive test during the first three keyframes after creation, that ensures that they are trackable and not wrongly triangulated, i.e due to spurious data association. A point must fulfill these two conditions:

- 1) The tracking must find the point in more than the 25% of the frames in which it is predicted to be visible.
- 2) If more than one keyframe has passed from map point creation, it must be observed from at least three keyframes.

Once a map point have passed this test, it can only be removed if at any time it is observed from less than three keyframes. This can happen when keyframes are culled and when local bundle adjustment discards outlier observations. This policy makes our map contain very few outliers.

C. New Map Points Creation

New map points are created by triangulating ORB from connected keyframes \mathcal{K}_c in the covisibility graph. For each

unmatched ORB in K_i we search a match with other unmatched point in other keyframe. This matching is done as explained in Section III-C and discard those matches that do not fulfill the epipolar constraint. ORB pairs are triangulated, and to accept the new points, positive depth in both cameras, parallax, reprojection error and scale consistency are checked. Initially a map point is observed from two keyframes but it could be matched in others, so it is projected in the rest of connected keyframes, and correspondences are searched as detailed in section V-D.

D. Local Bundle Adjustment

The local bundle adjustment optimizes the currently processed keyframe K_i , all the keyframes connected to it in the covisibility graph \mathcal{K}_c , and all the map points seen by those keyframes. All other keyframes that see that points but are not connected to the currently processed keyframe are included in the optimization but remain fixed. We use the Levenberg-Marquadt method implemented in g2o [33], and the Huber robust cost function. Observations that are marked as outliers are discarded at the middle and at the end of the optimization.

E. Local Keyframes Culling

In order to maintain a compact reconstruction, the local mapping tries to detect redundant keyframes and delete them. This is beneficial as bundle adjustment complexity is cubic in the number of keyframes, but also because it enables lifelong operation in the same environment as the number of keyframes will not grow unbounded, unless the visual content in the scene changes. We discard all the keyframes in \mathcal{K}_c whose 90% of the map points have been seen in at least other three keyframes in the same or finer scale. The scale condition ensures that map points maintain keyframes from which they are measured with most accuracy. This policy was inspired by the one proposed in the work of Tan et. al [22], where keyframes were discarded after a process of change detection.

VII. LOOP CLOSING

The loop closing thread takes K_i , the last keyframe processed by the local mapping, and tries to detect and close loops. The steps are next described.

A. Loop Candidates Detection

At first we compute the similarity between the bag of words vector of K_i and all its neighbors in the covisibility graph ($\theta_{\text{min}} = 30$) and retain the lowest score s_{min} . Then we query the recognition database and discard all those keyframes whose score is lower than s_{min} . This is a similar operation to gain robustness as the normalizing score in DBow2, which is computed from the previous image, but here we use covisibility information. In addition all those keyframes directly connected to K_i are discarded from the results. To accept a loop candidate we must detect consecutively three loop candidates that are consistent (keyframes connected in the covisibility graph). There can be several loop candidates if there are several places with similar appearance to K_i .

B. Compute the Similarity Transformation

In monocular SLAM there are seven degrees of freedom in which the map can drift, three translations, three rotations and a scale factor [5]. Therefore to close a loop we need to compute a similarity transformation from the current keyframe K_i to the loop keyframe K_l that informs us about the error accumulated in the loop. The computation of this similarity will serve also as geometrical validation of the loop.

We first compute correspondences between ORB associated to map points in the current keyframe and the loop candidate keyframes, following the procedure explained in section III-C. At this point we have 3D to 3D correspondences for each loop candidate. We alternatively perform RANSAC iterations with each candidate, trying to find a similarity transformation using the method of [38]. If we find a similarity S_{il} with enough inliers, we optimize it and perform a guided search of more correspondences. We optimize it again and, if S_{il} is supported by enough inliers, the loop with K_l is accepted.

C. Loop fusion

The first step in the loop correction is to fuse duplicated map points and insert new edges in the covisibility graph that will attach the loop closure. At first the current keyframe pose T_{iw} is corrected with the similarity transformation S_{il} and this correction is propagated to all the neighbors of K_i , concatenating transformations, so that both sides of the loop get aligned. All map points seen by the loop keyframe and its neighbors are projected into K_i and its neighbors and matches are searched in a narrow area from the projection, as done in section V-D. All those map points matched and those that were inliers in the computation of S_{il} are fused. All keyframes involved in the fusion will update their edges in the covisibility graph effectively creating edges that attach the loop closure.

D. Essential Graph optimization

To effectively close the loop, we perform a pose graph optimization over the *Essential Graph*, described in Section III-B, that distributes the loop closing error along the graph. The optimization is performed with g2o over similarity transformations to correct the scale drift as explained in [5]. After the optimization each map point is transformed according to the correction of one of the keyframes that observes it.

VIII. EXPERIMENTS

We have performed an extense experimental validation of our system in the large full robot sequence of NewCollege [35], evaluating the general performance of the system, in 16 hand-held indoor sequences of the TUM RGB-D benchmark [39], evaluating the localization accuracy, relocalization and lifelong capabilities, and in 10 car outdoor sequences from the KITTI dataset [36], evaluating real-time large scale operation and localization accuracy.

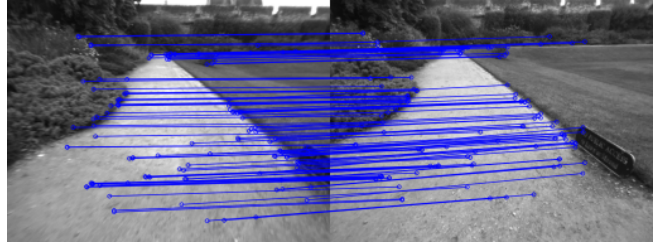


Fig. 3. Example of loop detected in the NewCollege sequence. We draw the inlier correspondences supporting the similarity transformation found.

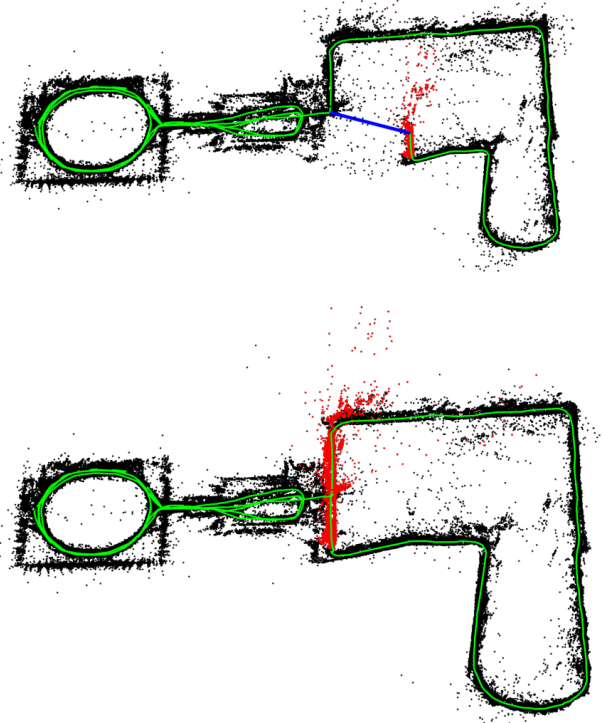


Fig. 4. Map before and after a loop closure in the NewCollege sequence. The loop closure match is drawn in blue, the trajectory in green, and the local map for the tracking at that moment in red. The local map is extended along both sides of the loop after it is closed.

A. System Performance in the NewCollege Dataset

The NewCollege dataset [35] contains a 2.2km sequence from a robot traversing a campus and adjacent parks. The sequence is recorded by a stereo camera at 20 fps and a resolution 512×382 . It contains several loops and fast rotations that makes the sequence quite challenging for monocular vision. To the best of our knowledge there is no other monocular system in the literature able to process this whole sequence. For example Strasdat et al. [6], despite being able to close loops and work in large scale environments, only showed monocular results for a small part of this sequence.

As an example of our loop closing procedure we show in Fig. 3 the detection of a loop with the inliers that support the similarity transformation. Fig. 4 shows the reconstruction before and after the loop closure. In red it is shown the local map, which after the loop closure extends along both sides of the loop closure. The whole map after processing the full

TABLE II
LOOP CLOSING TIMES IN NEWCOLLEGE

Loop	KeyFrames	Essential Graph Edges	Loop Detection (ms)		Loop Correction (s)		Total (s)
			Candidates Detection	Similarity Transformation	Fusion	Essential Graph Optimization	
1	287	1347	4.71	20.77	0.20	0.26	0.51
2	1082	5950	4.14	17.98	0.39	1.06	1.52
3	1279	7128	9.82	31.29	0.95	1.26	2.27
4	2648	12547	12.37	30.36	0.97	2.30	3.33
5	3150	16033	14.71	41.28	1.73	2.80	4.60
6	4496	21797	13.52	48.68	0.97	3.62	4.69

TABLE I
TRACKING AND MAPPING TIMES IN NEWCOLLEGE

Thread	Operation	Median (ms)	Mean (ms)	Std (ms)
TRACKING	ORB extraction	11.10	11.42	1.61
	Initial Pose Est.	3.38	3.45	0.99
	Track Local Map	14.84	16.01	9.98
	Total	30.57	31.60	10.39
LOCAL MAPPING	KeyFrame Insertion	10.29	11.88	5.03
	Map Point Culling	0.10	3.18	6.70
	Map Point Creation	66.79	72.96	31.48
	Local BA	296.08	360.41	171.11
	KeyFrame Culling	8.07	15.79	18.98
	Total	383.59	464.27	217.89

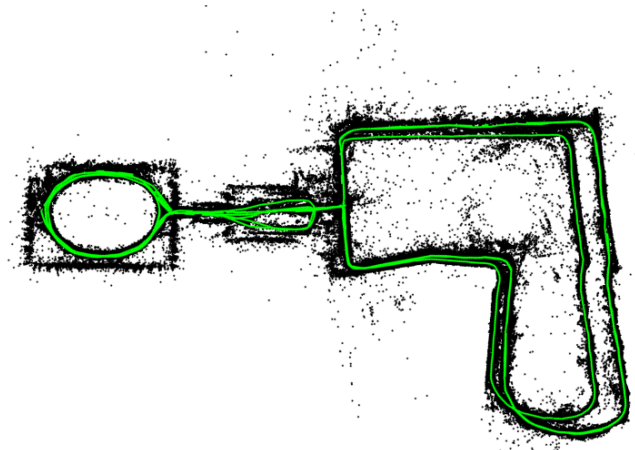


Fig. 5. ORB-SLAM reconstruction from the full sequence of NewCollege. The bigger loop on the right is traversed in opposite directions without possibility of closing loops and therefore they do not perfectly align.

sequence at its real frame-rate is shown in Fig. 5. The big loop on the right does not perfectly align because it was traversed in opposite directions and it was not possible to find visual loop closures.

We have extracted statistics of the times spent by each thread in this experiment. Table I shows the results for the tracking and the local mapping. Tracking works at frame-rates around 25-30Hz, being the most demanding task to track the local map. If needed this time could be reduced limiting the number of keyframes that are included in the local map. In the local mapping thread the most demanding task is local bundle adjustment. The local BA time varies if the robot is exploring or in a well mapped area, because during exploration bundle adjustment is interrupted if tracking inserts a new keyframe, as explained in section V-E. In case of not needing new keyframes local bundle adjustment performs a generous number of prefixed iterations.

Table II shows the results for each of the 6 loop closures found. It can be seen how the loop detection increases sublinearly with the number of keyframes. This is due to the efficient querying of the database that only compare the subset of images with words in common, which demonstrates the potential of bag of words for place recognition. Our *Essential Graph* includes edges around 5 times the number of keyframes, which is a quite sparse graph.

B. Localization accuracy in the TUM RGB-D Benchmark

The TUM RGB-D benchmark [39] is an excellent dataset to evaluate the accuracy of camera localization as it provides several sequences with accurate ground truth obtained with an external motion capture system. We have discarded all those sequences that we consider that are not suitable for pure monocular SLAM systems, as they contain strong rotations, no texture or no motion. All selected sequences have been preundistorted with the calibration provided and played at its real frame-rate.

For comparison we have also executed the novel, direct, semi-dense LSD-SLAM [8] and PTAM [3] in the benchmark. We compare also with the trajectories generated by RGBD-SLAM [40] which are provided for some of the sequences in the benchmark website. In order to compare ORB-SLAM, LSD-SLAM and PTAM with the ground truth we align the keyframe trajectories using a similarity transformation, as scale is unknown, and measure the absolute RMSE error [39]. In the case of RGBD-SLAM we align the trajectories with a rigid body transformation, but also a similarity to check if the scale was well recovered. LSD-SLAM initializes from random depth values, so we have discarded the first 10 keyframes when comparing with the ground truth. For PTAM we manually selected two frames from which we get a good initialization.

Table III shows the median results over 5 executions in each of the 16 sequences selected.

It can be seen that ORB-SLAM is able to process all the sequences, except for *fr3_nostructure_texture_far* (*fr3_nstr_tex_far*). This is a planar scene that because of the camera trajectory with respect to the plane has two possible interpretations, i.e. the twofold ambiguity described in [25]. Our initialization method detects the ambiguity and for safety refuses to initialize. PTAM initializes selecting sometimes the true solution and others the corrupted one, in which case the error is unacceptable. We have not noticed two different reconstructions from LSD-SLAM but the error in this sequence is very high. In the rest of the sequences, PTAM and LSD-SLAM exhibit less robustness than our method, loosing track in eight and three sequences respectively.

In terms of accuracy ORB-SLAM and PTAM are similar in open trajectories, while ORB-SLAM achieves higher accuracy when detecting large loops as in the sequence *fr3_nostructure_texture_near_with_loop* (*fr3_nstr_tex_near*). The most surprising results is that both PTAM and ORB-SLAM are clearly more accurate than LSD-SLAM and RGBD-SLAM. One of the possible causes can be that they reduce the map optimization to a pose-graph optimization were sensor measurements are discarded, while we perform bundle adjustment and jointly optimize cameras and map over sensor measurements, which is the gold standard algorithm to solve structure from motion [2]. We further discuss this result in Section IX-B. Another interesting result is that LSD-SLAM seems to be less robust to dynamic objects than our system as seen in *fr2_desk_with_person* and *fr3_walking_xyz*. Finally we have noticed that RGBD-SLAM has a bias in the scale in *fr2* sequences as aligning the trajectories with 7 DoF significantly reduces the error.

C. Relocalization Experiments in the TUM RGB-D benchmark

We perform two relocalization experiments in the TUM RGB-D benchmark. In the first experiment we build a map with the first 30 second of the sequence *fr2_xyz* and perform global relocalization with every successive frame and evaluate the accuracy of the recovered poses. We perform the same experiment with PTAM for comparison. Fig. 6 shows the keyframes used to create the initial map, the poses of the relocalised frames and the ground truth for those frames. It can be seen that PTAM is only able to relocalise frames which are near to the keyframes due to the little invariance of its relocalization method. Table IV shows the recall and the error with respect to the ground truth. ORB-SLAM accurately relocalise more than the double of frames than PTAM. In the second experiment we create an initial map with sequence *fr3_sitting_xyz* and try to relocalise all frames from *fr3_walking_xyz*. This is a challenging experiment as there are big occlusions due to people moving in the scene. Here PTAM finds no relocalizations while our system relocalizes 78% of the frames, as can be seen in Table IV. Fig. 7 shows some examples of challenging relocalizations performed by our system in these experiments.

TABLE III
KEYFRAME LOCALIZATION ERROR COMPARISON IN THE TUM RGB-D BENCHMARK [39]

	ATE RMSE (cm)			
	ORB-SLAM	PTAM	LSD-SLAM	RGBD-SLAM
fr1_xyz	0.90	1.15	9.00	1.34 (1.34)
fr2_xyz	0.30	0.20	2.15	2.61 (1.42)
fr1_floor	2.99	X	38.07	3.51 (3.51)
fr1_desk	1.69	X	10.65	2.58 (2.52)
fr2_360_kidnap	3.81	2.63	X	393.3 (100.5)
fr2_desk	0.88	X	4.57	9.50 (3.94)
fr3_long_office	3.45	X	38.53	-
fr3_nstr_tex_far	ambiguity detected*	4.92 / 34.74*	18.31	-
fr3_nstr_tex_near	1.39	2.74	7.54	-
fr3_str_tex_far	0.77	0.93	7.95	-
fr3_str_tex_near	1.58	1.04	X	-
fr2_desk_person	0.63	X	31.73	6.97 (2.00)
fr3_sit_xyz	0.79	0.83	7.73	-
fr3_sit_halfsph	1.34	X	5.87	-
fr3_walk_xyz	1.24	X	12.44	-
fr3_walk_halfsph	1.74	X	X	-

Results for ORB-SLAM, PTAM and LSD-SLAM are the median over 5 executions in each sequence. The trajectories have been aligned with 7DoF with the ground truth. Trajectories for RGBD-SLAM are taken from the benchmark website, only available for fr1 and fr2 sequences, and have been aligned with 6DoF and 7DoF (results between brackets). X means that the tracking is lost at some point and a significant portion of the sequence is not processed by the system. *In the sequence *fr3_nostructure_texture_far* the camera follows a trajectory with respect to the plane that yields a twofold ambiguity solution that is detected by our initialization method, which safely refuses the initialization. PTAM initializes sometimes from the true solution and others from the wrong one, which correspond to the lowest and highest errors shown respectively. In the case of LSD-SLAM we have not noticed two different initial reconstructions and we only show one result.

D. Lifelong Experiment in the TUM RGB-D Benchmark

Previous relocalization experiments have shown that our system is able to localize in a map from very different viewpoints and robustly under moderate dynamic changes. This property in conjunction with our keyframe culling procedure allows to operate lifelong in the same environment under different viewpoints and some dynamic changes.

In the case of a completely static scenario our system is able to maintain the number of keyframes bounded even if the camera is looking at the scene from different viewpoints. We demonstrate it in a custom sequence were the camera is looking at the same desk during 93 seconds but performing

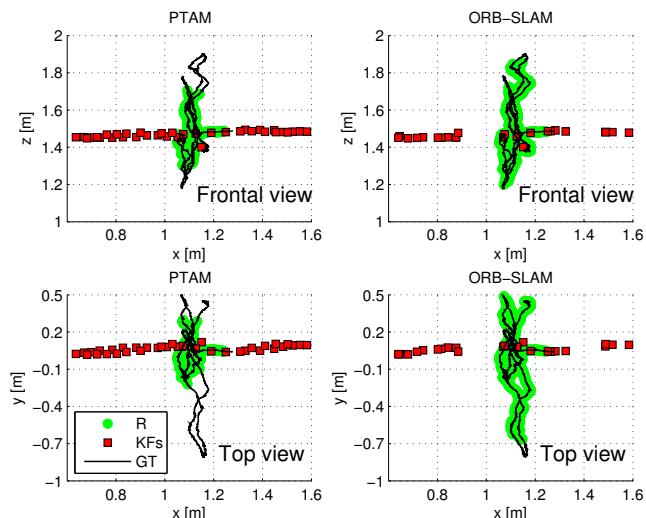


Fig. 6. Relocalization experiment in *fr2_xyz*. Map is initially created during the first 30 seconds of the sequence (KFs). The goal is to relocalise subsequent frames. Successful relocalizations (R) of our system and PTAM are shown. The ground truth (GT) is only shown for the frames to relocalise.

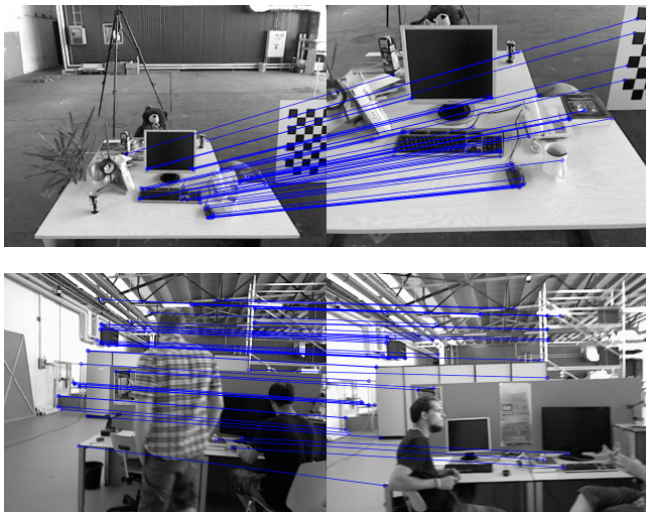


Fig. 7. Example of challenging relocalizations (severe scale change, dynamic objects) that our system successfully found in the relocalization experiments.

a trajectory so that the viewpoint is always changing. We compare the evolution of the number of keyframes in our map and those generated by PTAM in Fig. 8. It can be seen how PTAM is always inserting keyframes, while our mechanism to prune redundant keyframes makes its number to saturate.

While the lifelong operation in a static scenario should be a requirement of any SLAM system, more interesting is the case where dynamic changes occur. We analyze the behavior of our system in such scenario by running consecutively the dynamic sequences from *fr3*: *sitting_xyz*, *sitting_halfsphere*, *sitting_rpy*, *walking_xyz*, *walking_halfsphere* and *walking_rpy*. All the sequences focus the camera to the same desk but perform different trajectories, while people are moving and change some objects like chairs. Fig. 9(a) shows the evolution of the total number of keyframes in the map, and Fig. 9(b) shows for each keyframe its frame of creation and destruction, showing

TABLE IV
RESULTS FOR THE RELOCALIZATION EXPERIMENTS

System	Initial Map		Relocalization		
	KFs	RMSE (cm)	Recall (%)	RMSE (cm)	Max. Error (cm)
<i>fr2_xyz</i> . 2769 frames to relocalise					
PTAM	37	0.19	34.9	0.26	1.52
ORB-SLAM	24	0.19	78.4	0.38	1.67
<i>fr3_walking_xyz</i> . 859 frames to relocalise					
PTAM	34	0.83	0.0	-	-
ORB-SLAM	31	0.82	77.9	1.32	4.95

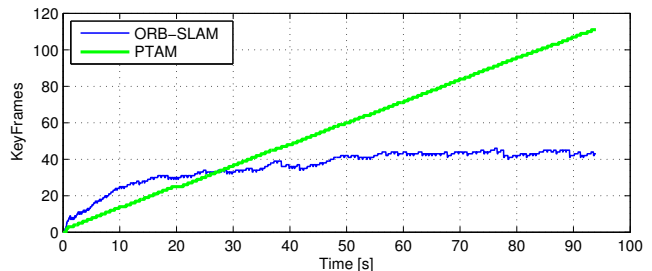
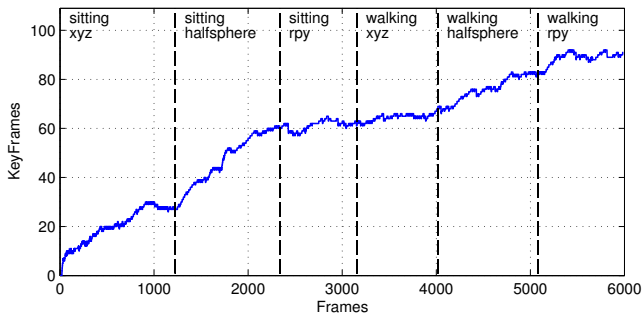


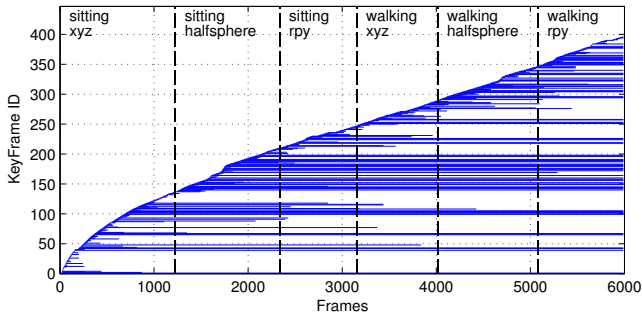
Fig. 8. Lifelong experiment in a static environment where the camera is always looking at the same place from different viewpoints. PTAM is always inserting keyframes, while ORB-SLAM is able to prune redundant keyframes and maintains a bounded-size map.

how long the keyframe have survived in the map. It can be seen that during the first two sequences the map size grows as all the views of the scene are being seen for the first time. In Fig. 9(b) we can see that several keyframes created during this two first sequences are maintained in the map during the whole experiment. During the sequences *sitting_rpy* and *walking_xyz* the map does not grow, because the map created so far explains well the scene. In contrast, during the last two sequences, more keyframes are inserted showing that there are some novelties in the scene that were not yet represented, due probably to dynamic changes. Finally Fig. 9(c) shows a histogram of the keyframes according to the time they have survived with respect to the remaining time of the sequence from its moment of creation. It can be seen that most of the keyframes are destroyed by the culling procedure soon after creation, and only a small subset survive until the end of the experiment. On one hand, this shows that our system has a generous keyframe spawning policy, which is very useful when performing abrupt motions in exploration. On the other hand the system is eventually able to select a small representative subset of those keyframes.

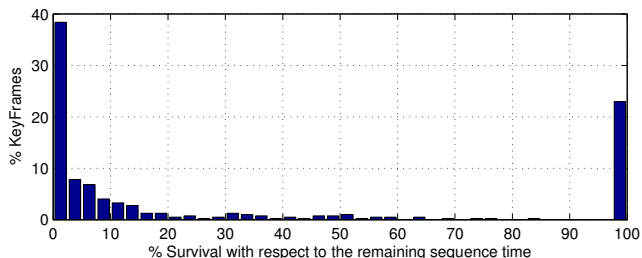
In these lifelong experiments we have shown that our map grows with the content of the scene but not with the time, and that is able to store the dynamic changes of the scene which could be useful to perform some scene understanding by accumulating experience in an environment.



(a) Evolution of the number of keyframes in the map



(b) Keyframe creation and destruction. Each horizontal line corresponds to a keyframe, from its creation frame until its destruction



(c) Histogram of the survival time of all spawned keyframes with respect to the remaining time of the experiment

Fig. 9. Lifelong experiment in a dynamic environment from the TUM RGB-D Benchmark.

E. Large Scale and Large Loop Closing in the KITTI Dataset

The odometry benchmark from the KITTI dataset [36] contains 11 sequences from a car driven around a residential area with accurate ground truth from GPS and a Velodyne laser scanner. This is a very challenging dataset for monocular vision due to fast rotations, areas with lot of foliage, which make more difficult data association, and relatively high car speed, being the sequences recorded at 10 fps. We play the sequences at the real frame-rate they were recorded and ORB-SLAM is able to process all the sequences by the exception of sequence 01 which is a highway with few trackable close objects. Sequences 00, 02, 05, 06, 07, 09 contain loops that were correctly detected and closed by our system. Sequence 09 contains a loop that can be detected only in a few frames at the end of the sequence, and our system not always detects it (the results provided are for the executions in which it was detected).

Qualitative comparisons of our trajectories and the ground truth are shown in Fig. 10 and Fig. 11. As in the TUM RGB-D

TABLE V
RESULTS OF OUR SYSTEM IN THE KITTI DATASET.

Sequence	Dimension (m×m)	ORB-SLAM		+ Global BA (20 its.)	
		KFs	RMSE (m)	RMSE (m)	Time BA (s)
KITTI 00	564 × 496	1391	6.68	5.33	24.83
KITTI 02	599 × 946	1801	21.75	21.28	30.07
KITTI 03	471 × 199	250	1.59	1.51	4.88
KITTI 04	0.5 × 394	108	1.79	1.62	1.58
KITTI 05	479 × 426	820	8.23	4.85	15.20
KITTI 06	23 × 457	373	14.68	12.34	7.78
KITTI 07	191 × 209	351	3.36	2.26	6.28
KITTI 08	808 × 391	1473	46.58	46.68	25.60
KITTI 09	465 × 568	653	7.62	6.62	11.33
KITTI 10	671 × 177	411	8.68	8.80	7.64

benchmark we have aligned the keyframe trajectories of our system and the ground truth with a similarity transformation. We can compare qualitatively our results from Fig. 10 and Fig. 11 with the results provided for sequences 00, 05, 06, 07 and 08 by the recent monocular SLAM approach of Lim et. al [23] in their figure 10. ORB-SLAM produces clearly more accurate trajectories for all those sequences by the exception of sequence 08 in which they seem to suffer less drift.

Table V shows the median RMSE error of the keyframe trajectory over five executions in each sequence. We also provide the dimensions of the maps to put in context the errors. The results demonstrate that our system is very accurate being the trajectory error typically around the 1% of its dimensions, sometimes less as in sequence 03 with an error of the 0.3% or higher as in sequence 08 with the 5%. In sequence 08 there are no loops and drift cannot be corrected, which makes clear the need of loop closures to achieve accurate reconstructions.

In this experiment we have also checked how much the reconstruction can be improved by performing a global bundle adjustment (20 iterations) at the end of each sequence including all keyframes and map points. We have noticed that some iterations of global BA slightly improves the accuracy in the trajectories with loops but it has negligible effect in open trajectories, which means that the output of our system is already very accurate. In any case if the most accurate results are needed our algorithm provides a set of matches, which define a strong camera network, and an initial guess, so that full BA converge in few iterations.

IX. CONCLUSIONS AND DISCUSSION

A. Conclusions

In this work we have presented a new monocular SLAM system with a detailed description of its building blocks and an exhaustive evaluation in public datasets. Our system has demonstrated that it can process sequences from indoor and outdoor scenes and from car, robot and hand-held motions. The accuracy of the system is typically below 1 cm in small

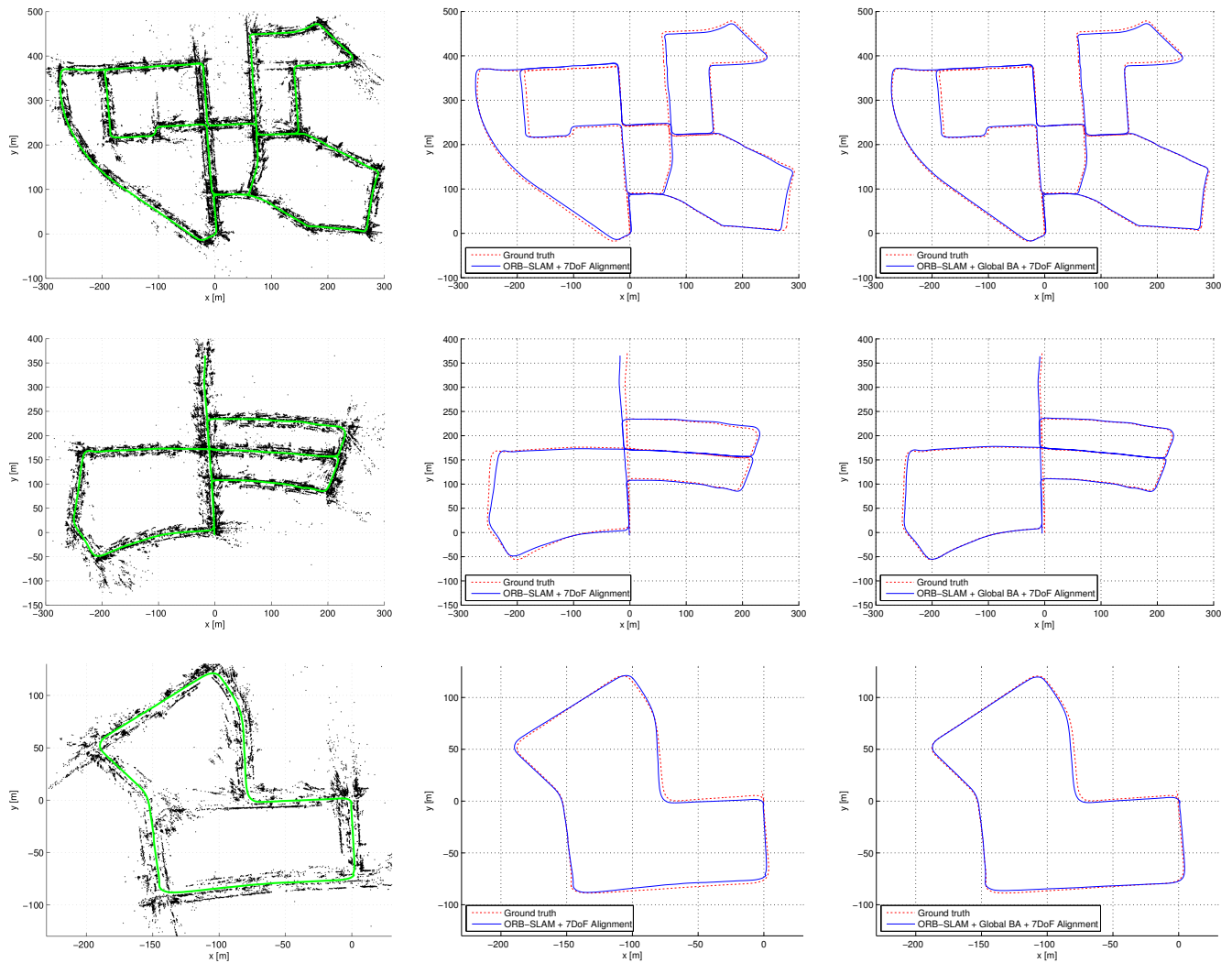


Fig. 10. Sequences 00, 05 and 07 from the odometry benchmark of the KITTI dataset. Left: points and keyframe trajectory. Center: trajectory and ground truth. Right: trajectory after 20 iterations of full BA. The output of our system is quite accurate, while it can be slightly improved with some iterations of BA.

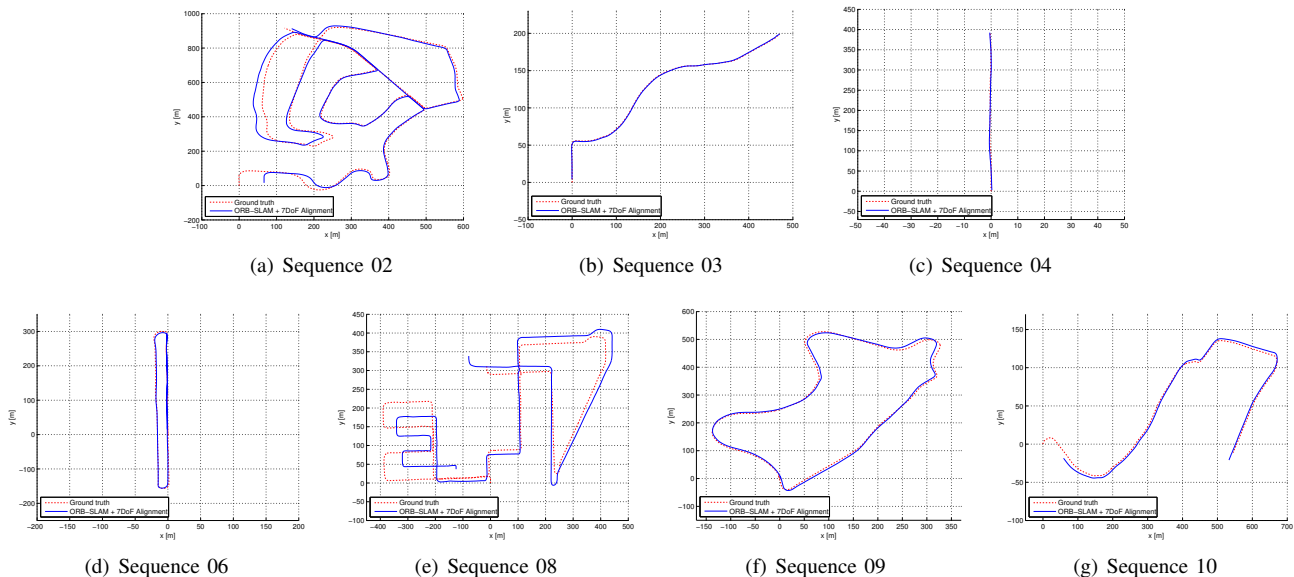


Fig. 11. ORB-SLAM keyframe trajectories in sequences 02, 03, 04, 06, 08, 09 and 10 from the odometry benchmark of the KITTI dataset. Sequence 08 does not contain loops and drift (especially scale) is not corrected.

indoor scenarios and of a few meters in large outdoor scenarios (once we have aligned the scale with the ground truth). Despite the maturity of monocular SLAM field, PTAM by Klein and Murray [3] is still considered today as the baseline, being the most accurate known reconstruction method from monocular video in real time. It is not coincidence that the backend of PTAM is bundle adjustment, which is well known to be the gold standard method for the offline Structure From Motion problem [2]. One of the main successes of PTAM was to bring that knowledge into the robotics SLAM community and demonstrate its real time performance. The main contribution of this work is to expand the versatility of PTAM to a new bunch of environments that were intractable for that system. To achieve this we have design from scratch a new Monocular SLAM system with some own ideas and algorithms, but also others from excellent works developed in the last years as the loop detection of Gálvez-López and Tardós [4], the loop closing procedure and covisibility graph of Strasdat et.al [5], [6], the optimization framework g2o by Kuemmerle et. al [33] and ORB features by Rubble et. al [7]. To the best of our knowledge no other system has demonstrated to work in such amount of different scenarios and with our accuracy, which makes our system the most reliable and complete solution for Monocular SLAM. Our novel policy to spawn and cull keyframes, permits to create temporary keyframes really useful in poorly conditioned exploration trajectories, i.e. close to pure rotations or fast movements, that are eventually removed when considered redundant. When operating lifelong in the same environment, this makes the map only grow if the visual content of the scene changes, and moreover it stores a history of its visual appearances. Interesting results could be obtained analyzing this history to infer some scene understanding.

Finally we have also demonstrated that ORB features have enough recognition power to enable place recognition from severe viewpoint change and they are so fast to extract and match (without needing multi-threading or GPU acceleration) that enable real time accurate tracking and mapping.

B. Sparse/Feature-based vs. Dense/Direct methods

Recently real-time Monocular SLAM algorithms as DTAM [41] and LSD-SLAM [8] have appeared, being able to perform dense or semi dense reconstructions of the environment, while the camera is localized optimizing directly over image pixel intensities. These direct approaches do not need to extract features and can avoid the corresponding artifacts, being clearly more robust to blur. In addition their denser reconstructions compared to the sparse point map of our system or PTAM, are more useful for other tasks than just camera localization.

However, apart from these benefits, direct methods have their own limitations. Firstly, these methods assume a surface reflectance model that in real scenes produces its own artifacts. These methods typically match pixels from a narrow baseline as the reflectance model is violated from wide baseline and many erroneous correspondences would appear. This has a great impact in reconstruction accuracy, which requires wide baseline observations to reduce depth uncertainty. Finally because direct methods are in general very computational

demanding, map is just incrementally expanded as in DTAM, or map optimization is reduced to a pose graph optimization, discarding all sensor measurements as in LSD-SLAM.

In contrast, feature-based methods are able to match features from wide baseline, thanks to their viewpoint invariance, and perform bundle adjustment that jointly optimize camera poses and points over sensor measurements. In the context of structure and motion estimation Torr and Zisserman [42] also pointed the benefits of feature-based against direct methods. In this work we show experimental evidence, see Section VIII-B, of the superior accuracy of feature-based methods in real-time SLAM. We consider that the future of Monocular SLAM should incorporate the best of both approaches and not only one perspective.

C. Future Work

The accuracy of our system could still be improved incorporating points at infinity in the tracking. These points, which are not seen with parallax and not included in the map, are very informative of the rotation of the camera [19], and could significantly improve tracking accuracy. To include these points an homogeneous representation should be used [1].

Another open way is to upgrade the sparse map of our system to a denser and more useful reconstruction as it was discussed above. Thanks to our keyframe selection, keyframes comprise a compact summary of the environment with a very high pose accuracy and rich information of covisibility. Therefore the ORB-SLAM sparse map can be an excellent initial guess and skeleton on top of which a dense and accurate map of the scene can be grown.

REFERENCES

- [1] B. Triggs, P. F. McLauchlan, R. I. Hartley, and A. W. Fitzgibbon, "Bundle adjustment a modern synthesis," in *Vision algorithms: theory and practice*, 2000, pp. 298–372.
- [2] R. Hartley and A. Zisserman, *Multiple View Geometry in Computer Vision*, 2nd ed. Cambridge University Press, 2004.
- [3] G. Klein and D. Murray, "Parallel tracking and mapping for small AR workspaces," in *IEEE and ACM International Symposium on Mixed and Augmented Reality (ISMAR)*, Nara, Japan, November 2007, pp. 225–234.
- [4] D. Gálvez-López and J. D. Tardós, "Bags of binary words for fast place recognition in image sequences," *IEEE Transactions on Robotics*, vol. 28, no. 5, pp. 1188–1197, 2012.
- [5] H. Strasdat, J. M. M. Montiel, and A. J. Davison, "Scale drift-aware large scale monocular SLAM," in *Robotics: Science and Systems (RSS)*, Zaragoza, Spain, June 2010.
- [6] H. Strasdat, A. J. Davison, J. M. M. Montiel, and K. Konolige, "Double window optimisation for constant time visual SLAM," in *IEEE International Conference on Computer Vision (ICCV)*, Barcelona, Spain, November 2011, pp. 2352–2359.
- [7] E. Rublee, V. Rabaud, K. Konolige, and G. Bradski, "ORB: an efficient alternative to SIFT or SURF," in *IEEE International Conference on Computer Vision (ICCV)*, Barcelona, Spain, November 2011, pp. 2564–2571.
- [8] J. Engel, T. Schöps, and D. Cremers, "LSD-SLAM: Large-scale direct monocular SLAM," in *European Conference on Computer Vision (ECCV)*, Zurich, Switzerland, September 2014, pp. 834–849.
- [9] R. Mur-Artal and J. D. Tardós, "Fast relocalisation and loop closing in keyframe-based SLAM," in *IEEE International Conference on Robotics and Automation (ICRA)*, Hong Kong, China, June 2014, pp. 846–853.
- [10] —, "ORB-SLAM: Tracking and mapping recognizable features," in *MVIGRO Workshop at Robotics Science and Systems (RSS)*, Berkeley, USA, July 2014.
- [11] B. Williams, M. Cummins, J. Neira, P. Newman, I. Reid, and J. D. Tardós, "A comparison of loop closing techniques in monocular SLAM," *Robotics and Autonomous Systems*, vol. 57, no. 12, pp. 1188–1197, 2009.

- [12] D. Nister and H. Stewenius, "Scalable recognition with a vocabulary tree," in *IEEE Computer Society Conference on Computer Vision and Pattern Recognition (CVPR)*, vol. 2, New York City, USA, June 2006, pp. 2161–2168.
- [13] M. Cummins and P. Newman, "Appearance-only SLAM at large scale with FAB-MAP 2.0," *The International Journal of Robotics Research*, vol. 30, no. 9, pp. 1100–1123, 2011.
- [14] M. Calonder, V. Lepetit, C. Strecha, and P. Fua, "BRIEF: Binary Robust Independent Elementary Features," in *European Conference on Computer Vision (ECCV)*, Hersonissos, Greece, September 2010, pp. 778–792.
- [15] E. Rosten and T. Drummond, "Machine learning for high-speed corner detection," in *European Conference on Computer Vision (ECCV)*, Graz, Austria, May 2006, pp. 430–443.
- [16] H. Bay, T. Tuytelaars, and L. Van Gool, "SURF: Speeded Up Robust Features," in *European Conference on Computer Vision (ECCV)*, Graz, Austria, May 2006, pp. 404–417.
- [17] D. G. Lowe, "Distinctive image features from scale-invariant keypoints," *International Journal of Computer Vision*, vol. 60, no. 2, pp. 91–110, 2004.
- [18] A. J. Davison, I. D. Reid, N. D. Molton, and O. Stasse, "MonoSLAM: Real-time single camera SLAM," *IEEE Transactions on Pattern Analysis and Machine Intelligence*, vol. 29, no. 6, pp. 1052–1067, 2007.
- [19] J. Civera, A. J. Davison, and J. M. M. Montiel, "Inverse depth parametrization for monocular SLAM," *IEEE Transactions on Robotics*, vol. 24, no. 5, pp. 932–945, 2008.
- [20] C. Forster, M. Pizzoli, and D. Scaramuzza, "SVO: Fast semi-direct monocular visual odometry," in *Proc. IEEE Intl. Conf. on Robotics and Automation*, Hong Kong, China, June 2014, pp. 15–22.
- [21] O. D. Faugeras and F. Lustman, "Motion and structure from motion in a piecewise planar environment," *International Journal of Pattern Recognition and Artificial Intelligence*, vol. 2, no. 03, pp. 485–508, 1988.
- [22] W. Tan, H. Liu, Z. Dong, G. Zhang, and H. Bao, "Robust monocular SLAM in dynamic environments," in *IEEE International Symposium on Mixed and Augmented Reality (ISMAR)*, Adelaide, Australia, October 2013, pp. 209–218.
- [23] H. Lim, J. Lim, and H. J. Kim, "Real-time 6-DOF monocular visual SLAM in a large-scale environment," in *IEEE International Conference on Robotics and Automation (ICRA)*, Hong Kong, China, June 2014, pp. 1532–1539.
- [24] D. Nistér, "An efficient solution to the five-point relative pose problem," *IEEE Transactions on Pattern Analysis and Machine Intelligence*, vol. 26, no. 6, pp. 756–770, 2004.
- [25] H. Longuet-Higgins, "The reconstruction of a plane surface from two perspective projections," *Proceedings of the Royal Society of London. Series B. Biological Sciences*, vol. 227, no. 1249, pp. 399–410, 1986.
- [26] P. H. Torr, A. W. Fitzgibbon, and A. Zisserman, "The problem of degeneracy in structure and motion recovery from uncalibrated image sequences," *International Journal of Computer Vision*, vol. 32, no. 1, pp. 27–44, 1999.
- [27] E. Eade and T. Drummond, "Scalable monocular SLAM," in *IEEE Computer Society Conference on Computer Vision and Pattern Recognition (CVPR)*, vol. 1, New York City, USA, June 2006, pp. 469–476.
- [28] H. Strasdat, J. M. M. Montiel, and A. J. Davison, "Visual SLAM: Why filter?" *Image and Vision Computing*, vol. 30, no. 2, pp. 65–77, 2012.
- [29] G. Klein and D. Murray, "Improving the agility of keyframe-based slam," in *European Conference on Computer Vision (ECCV)*, Marseille, France, October 2008, pp. 802–815.
- [30] D. Scaramuzza, M. Achtelik, L. Doitsidis, F. Fraundorfer, E. Kosmatopoulos, A. Martinelli, M. Achtelik, M. Chli, S. Chatzichristofis, L. Kneip, et al., "Vision-controlled micro flying robots: from system design to autonomous navigation and mapping in GPS-denied environments," *IEEE Robotics & Automation Magazine*, pp. 1–10, 2013.
- [31] J. Engel, J. Sturm, and D. Cremers, "Scale-aware navigation of a low-cost quadcopter with a monocular camera," *Robotics and Autonomous Systems*, vol. 62, no. 11, pp. 1646–1656, 2014.
- [32] K. Pirker, M. Ruther, and H. Bischof, "CD SLAM-continuous localization and mapping in a dynamic world," in *IEEE/RSJ International Conference on Intelligent Robots and Systems (IROS)*, San Francisco, USA, September 2011, pp. 3990–3997.
- [33] R. Kuemmerle, G. Grisetti, H. Strasdat, K. Konolige, and W. Burgard, "g2o: A general framework for graph optimization," in *IEEE International Conference on Robotics and Automation (ICRA)*, Shanghai, China, May 2011, pp. 3607–3613.
- [34] R. Szeliski, *Computer vision: algorithms and applications*. Springer, 2010.
- [35] M. Smith, I. Baldwin, W. Churchill, R. Paul, and P. Newman, "The new college vision and laser data set," *The International Journal of Robotics Research*, vol. 28, no. 5, pp. 595–599, 2009.
- [36] A. Geiger, P. Lenz, C. Stiller, and R. Urtasun, "Vision meets robotics: The KITTI dataset," *The International Journal of Robotics Research*, vol. 32, no. 11, pp. 1231–1237, 2013.
- [37] V. Lepetit, F. Moreno-Noguer, and P. Fua, "EPnP: An accurate O(n) solution to the PnP problem," *International Journal of Computer Vision*, vol. 81, no. 2, pp. 155–166, 2009.
- [38] B. K. P. Horn, "Closed-form solution of absolute orientation using unit quaternions," *Journal of the Optical Society of America A*, vol. 4, no. 4, pp. 629–642, 1987.
- [39] J. Sturm, N. Engelhard, F. Endres, W. Burgard, and D. Cremers, "A benchmark for the evaluation of RGB-D SLAM systems," in *IEEE/RSJ International Conference on Intelligent Robots and Systems (IROS)*, Vilamoura, Portugal, October 2012, pp. 573–580.
- [40] F. Endres, J. Hess, N. Engelhard, J. Sturm, D. Cremers, and W. Burgard, "An evaluation of the RGB-D SLAM system," in *IEEE International Conference on Robotics and Automation (ICRA)*, Saint Paul, USA, May 2012, pp. 1691–1696.
- [41] R. A. Newcombe, S. J. Lovegrove, and A. J. Davison, "DTAM: Dense tracking and mapping in real-time," in *IEEE International Conference on Computer Vision (ICCV)*, Barcelona, Spain, November 2011, pp. 2320–2327.
- [42] P. H. Torr and A. Zisserman, "Feature based methods for structure and motion estimation," in *Vision Algorithms: Theory and Practice*. Springer, 2000, pp. 278–294.